Brain & Development 41 (2019) 85–95

BRAIN & DEVELOPMENT
Official Journal of the Japanese Society of Child Neurology

www.elsevier.com/locate/braindev

Original article

Clasmatodendrosis is associated with dendritic spines and does not represent autophagic astrocyte death in influenza-associated encephalopathy

Masaya Tachibana [a,b], Ikuko Mohri [a,b], Ikuko Hirata [a,b], Ayano Kuwada [a,b], Shihoko Kimura-Ohba [b], Kuriko Kagitani-Shimono [a,b], Hiroaki Fushimi [c], Takeshi Inoue [d], Masashi Shiomi [d], Yukio Kakuta [e], Makoto Takeuchi [f], Shigeo Murayama [g], Masahiro Nakayama [f], Keiichi Ozono [b], Masako Taniike [a,b,*]

[a] *Department of Child Development, Osaka University United Graduate School of Child Development, Suita, Osaka, Japan*
[b] *Department of Pediatrics, Osaka University Graduate School of Medicine, Suita, Osaka, Japan*
[c] *Department of Pathology, Osaka General Medical Center, Osaka, Japan*
[d] *Department of Pathology, Osaka City General Hospital, Osaka, Japan*
[e] *Department of Pathology, Japan Organization of Occupational Health and Safety, Yokohama Rosai Hospital, Yokohama, Kanagawa, Japan*
[f] *Division of Clinical Laboratory Medicine and Anatomic Pathology, Osaka Medical Center and Research Institute for Maternal and Child Health, Izumi, Osaka, Japan*
[g] *Tokyo Metropolitan Institute of Gerontology, Tokyo, Japan*

Received 26 March 2018; received in revised form 2 July 2018; accepted 13 July 2018

Abstract

Background: Influenza-associated encephalopathy (IAE) is one of the most serious CNS complications of an influenza virus infection, with unclear pathophysiology. Clasmatodendrosis is a complex of morphological changes in astrocytes characterized by fragmentation of the distal processes and swollen cell bodies. Although pathologists in Japan have long been aware of the presence of clasmatodendrosis in IAE brains, no details of the phenomenon have been published to date. We aimed to confirm the existence, and characterize the spatial distribution of clasmatodendrosis in postmortem IAE brains.

Methods: Autopsied brains from 7 patients with IAE and 8 non-IAE subjects were examined immunohistochemically. In addition, immunofluorescent staining and electron microscopy were performed.

Results: Clasmatodendrosis was present in all examined regions of the IAE brains, but none of the control brains. Fragmented processes of astrocytes in IAE brains were closely adjacent to synapses on the dendritic spines, with the fragmentation especially prominent in the cerebellar molecular layer. In addition, the clasmatodendrotic astrocytes were negative for autophagy markers. Furthermore, whereas aquaporin 4 was predominantly detected in the perivascular endfeet of astrocytes in the control brains, its primary localization site shifted to the fragmented perisynaptic processes in the IAE brains.

Conclusion: Clasmatodendrosis was distributed diffusely in the IAE brains in close association with synapses, and was not caused by astrocyte autophagy. Clasmatodendrosis may be a suggestive pathological feature of IAE.

Keywords: Influenza-associated encephalopathy; Clasmatodendrosis; Astrocytes; Synapses; Autophagy; Aquaporin4

* Corresponding author at: Department of Child Development, Osaka University United Graduate School of Child Development, 2-2 Yamadaoka, Suita, Osaka 565-0871 Japan. Tel./fax: 06-6879-3863.
E-mail address: masako@kokoro.med.osaka-u.ac.jp (M. Taniike).

https://doi.org/10.1016/j.braindev.2018.07.008
0387-7604/

1. Introduction

Influenza-associated encephalopathy (IAE) and encephalitis are one of the most severe CNS complications of influenza infections [1,2]. In Japan, 100–350 cases of IAE are reported annually, with a mortality rate as high as 20–30% before 2000 [3,4]. Until recently, IAE had been reported almost exclusively in children from Japan or other Asian countries, and rarely documented in Western countries. However, during the worldwide epidemic of the new H1N1 influenza strain in 2009, several cases of IAE were reported globally and showed the same clinical characteristics as those in Japan [5,6]. Recently, the IAE mortality rate has remarkably decreased to 7% [7] because of progress in early-phase intensive care; however, IAE survivors still experience severe brain damage [8]. Although few postmortem brain samples are available, their detailed pathological investigation is required for the prevention and alleviation of IAE.

Postmortem neuropathological examination of IAE specimens revealed cerebral edema and the breakdown of the blood-brain barrier (BBB) due to the destruction of endothelial cells [3]. It is now widely accepted that the virus itself rarely invades the CNS but, rather, induces its central neurological effects indirectly, via proinflammatory cytokines such as interleukin-6 and tumor necrosis factor-α [3,9]. However, the detailed sequence of the pathophysiological events underlying IAE development remains unclear.

Clasmatodendrosis refers to abnormal morphological changes in astrocytes including the disintegration of the distal processes, and the swelling and vacuolation of the cell body [9]. Clasmatodendrosis has been reported to occur in the white matter (WM) lesions in Alzheimer's and cerebrovascular diseases [10], periventricular zones of patients with mixed dementia [11], corpus callosum during chronic cerebral hypoperfusion in mice [12], and hippocampuses of rats with experimental chronic epilepsy [13]. It is common knowledge among Japanese pathologists that clasmatodendrosis is also observable in the WM of IAE patients, even though such astrocytic changes have so far been documented only briefly in a limited number of IAE case reports [14,15]. The spatial distribution of clasmatodendrosis and its pathophysiological significance remain to be clarified.

Severe IAE cases are classified, mostly based on clinical signs and symptoms, into 3 categories: Reye's syndrome, acute necrotizing encephalopathy (ANE), and hemorrhagic shock and encephalopathy (HSE) syndrome [3]. It remains unclear whether clasmatodendrosis occurs in specific subtypes of IAE or is a feature of any rapidly progressive IAE.

Recently, involvement of the autophagy-lysosome pathway in clasmatodendrosis has been reported in rat models of status epilepticus [16,17], while earlier reports described clasmatodendrosis as coagulative necrotic cell death [18,19]. However, autophagy in IAE-associated clasmatodendrosis has not been explored yet.

Previous studies documented altered distributions of aquaporin 4 (AQP4) in clasmatodendrosis in post-stroke dementia [20] and an animal model of hypoperfusion [12]. While the majority of AQP4 is localized in astrocytic endfeet around the vessels and pia mater in the normal brain, AQP4 is also present in perisynaptic astrocytic processes, where it mediates activity-dependent water fluxes from the synapse into the astrocyte [21]. The water is then siphoned into the blood or cerebrospinal fluid through perivascular AQP4 [21]. No studies to date have examined AQP4 localization in IAE brains.

In the present study, we investigated the morphological changes in astrocytes and their spatial distribution in the postmortem brains of IAE patients by immunohistochemistry and electron microscopy. We also compared the localization of AQP4 in astrocytes between IAE and control brains, and examined the expression of autophagic markers in clasmatodendrotic astrocytes in IAE. Our findings suggest that clasmatodendrosis could be a highly suggestive pathological feature of IAE.

2. Materials and methods

2.1. Tissues

Human brain tissues were obtained from the Osaka Medical Center and Research Institute for Maternal and Child Health, Osaka General Medical Center, Osaka City General Hospital, and Tokyo Metropolitan Geriatric Hospital and Institute of Gerontology. The brains of 7 IAE patients (died in 1989–2003) and 8 controls (died in 1997–2009) were examined. The control brains were from subjects who showed no clinical evidence of IAE or other neurological involvement in the cause of death or comorbidities. Among the 7 IAE cases, the diagnosis in the 3 recent cases ("influenza #1, 2, and 5") was confirmed by direct detection of influenza virus antigen. In the older 4 cases (influenza #3, 4, 6, and 7), the diagnosis was based exclusively on the clinical course and concurrence with an influenza epidemic. Subject details are listed in Table 1. The age of the subjects with IAE and non-IAE controls ranged from 21 months to 13 years (mean, 4.5 years), and from 2 months to 14 years (mean, 5.8 years), respectively. The brains from all IAE subjects were heavy and showed extensive diffuse edema. In contrast, only some control subjects that died from bacterial encephalitis and hemophagocytic syndrome had relatively heavy brains with focal brain edema (Table 2). The mean brain weight at autopsy was 1318 g (877–1669 g) in the IAE group and 1023 g (460–1414 g) in the non-IAE group. In all cases, autopsy was performed after written

Table 1
Profiles of patients.

Case No.	Age	Sex	Cause of Death	Co-Morbidities	PMI (hours)	Brain Weight (g)	Symptom Onset to Death (hours)
influenza #1	13y1m	M	IAE (HSE)	tuberous sclerosis	1.5	1200	12.5
influenza #2	1y9m	M	IAE (Rye's)	CHARGE syndrome	12.0	877	26
influenza #3	5y1m	F	IAE (Rye's)[§]		1.5	1360	36
influenza #4	3y2m	M	IAE (HSE)[§]		13.0	1669	26
influenza #5	1y11m	M	IAE (ANE)		1.5	1350	51
influenza #6	3y1m	M	IAE (HSE)[§]		4.5	1390	34
influenza #7	3y7m	M	IAE (HSE)[§]		12.5	1380	24
control #1	2y6m	F	acute liver failure	Down's syndrome, TOF	2.0	870	
control #2	14y6m	F	sudden death, pulmonary hemorrhage	VSD	1.5	1171	
control #3	2m	M	myocarditis		1.5	460	
control #4	11m	M	pulmonary hypertension	ELBW, liver cirrhosis	2.0	540	
control #5	4y9m	M	septic shock	neuroblastoma, post-chemotherapy	1.5	1025	
control #6	2y9m	M	bacterial encephalitis, pulmonary suppuration		2.5	1370	
control #7	10y4m	F	HPS	acute myeloid leukemia	1.2	1337	
control #8	11y3m	M	HPS	neumonia (adeno virus7), Henoch-Shönlein purpura	11.8	1414	

PMI, postmortem interval to autopsy; IAE, Influenza Associated Encephalopathy; HSE, hemorrhagic shock and encephalopathy; Rye's, Rye's syndrome; ANE, acute necrotizing encephalopathy; CHRAGE, Coloboroma of Iris, Heart disease, Atresia choanae, Retarded growth and mental development, Genital hypoplasia, Ear anomalies and deafness; TOF, Tetralogy of Fallot; VSD, Ventricular Septal Defect; ELBW, Extremely Low Birth Weight; HPS, hemophagocytic syndrome. [§]IAE diagnosed by clinical course but not confirmed by virus detection.

informed consent had been obtained from the parents. This study was approved by the Institutional Review Board of Osaka University Hospital.

2.2. Tissue processing

Tissues obtained at autopsy were immediately fixed in 10% formalin and further processed into paraffin blocks. Five-micrometer-thick paraffin sections of the frontal cortex and cerebellum were used for immunohistochemical studies. In addition, tissue blocks were cut from the formalin-fixed tissues from 2 IAE cases (influenza #1, 2) and 2 control cases (control #1, 2), and sliced into 50-μm-thick free-floating sections by a vibrating-blade microtome (LEICA VT 1000s, Leica Microsystems GmbH, Wetzler, Germany). Sections from influenza case #1 were used after ascertaining that they contained no tubers or areas of calcification.

2.3. Immunohistochemistry

The following primary antibodies were used: rabbit polyclonal anti-cow glial fibrillary acidic protein (GFAP; DAKO, Cambridgeshire, UK; diluted 1:1,000), mouse monoclonal anti-GFAP (Abcam, Cambridge, MA, USA; diluted 1:2,000), mouse monoclonal anti-microtubule-associated protein 2 (MAP2; Abcam; diluted 1:1,000), mouse monoclonal anti-neurofilament phosphorylated (SMI-31; Covance, Emeryville, CA, USA; diluted 1:1,000), rabbit anti-synaptophysin (SYP; Zymed Lab., San Francisco, CA, USA; diluted 1:200), rabbit polyclonal anti-p62/SQSTM1 (MBL, Nagoya, Japan; diluted 1:500), rabbit anti-microtubule-associated protein 1 light chain 3 (LC3; MBL; diluted 1:500), mouse anti-CD68 (DAKO; diluted 1:100), and rabbit polyclonal anti-AQP4 (Santa Cruz Biotechnology Inc., Santa Cruz, CA, USA; diluted 1:100).

Deparaffinized sections and floating sections were preincubated with 0.3% H_2O_2 in methanol and microwaved in 10 mM citrate buffer (pH 6.0) for 60 min or pretreated with 0.1% trypsin at 37 °C for 15 min for antigen retrieval. Then the sections were sequentially incubated in PBS containing 0.3% Triton X-100 and 5% normal goat serum, primary antibody, or biotinylated secondary antibody (Vector Laboratories Inc., Burlingame, CA, USA; 2 μg/mL) with avidin and biotinylated horseradish peroxidase macromolecular complex (ABC; ABC kit, Vector Laboratories Inc.) according to the manufacturer's protocol. The staining was visualized with 3,3′-diaminobenzidine (DAB). The specificity of immunostaining was confirmed by omitting the primary antibody. The stained sections were observed on a BX51 microscope equipped with a DP50 digital camera (Olympus Co., Tokyo, Japan).

Table 2
Astroglial morphology and activation status in IAE and control brains.

Case No.	Cause of Death	Cerebrum (Frontal Cortex)	Cerebellum	Hippocampus	Splenium of Corpus Callosum	Thalamus
influenza #1	IAE (HSE)	C	C	C	C	C
influenza #2	IAE (Rye)	C	C	–	–	C
influenza #3	IAE (Rye)	C	C	–	–	C
influenza #4	IAE (HSE)	C	C	C	–	C
influenza #5	IAE (ANE)	C	C	C	–	C
influenza #6	IAE (HSE)	C	C	C	–	C
influenza #7	IAE (HSE)	C	C	C	–	C
control #1	acute liver failure	N	N	N	N	N
control #2	sudden death pulmonary hemorrhage	N	N	–	–	N
control #3	myocarditis	A	A	–	–	–
control #4	pulmonary hypertension	N	N	N	–	N
control #5	sepsis	A	A	A	–	A
control #6	bacterial encephalitis	A	A	A	–	A
control #7	hemophagocytic syndrome	A	A	–	–	–
control #8	hemophagocytic syndrome	A	A	–	–	–

C, clasmatodendrosis; A, activated astrocytes without clasmatodendrosis; N, no activation of astrocytes or no clasmatodendrosis; –, not available/examined. IAE, influenza-associated encephalopathy; HSE, hemorrhagic shock and encephalopathy; ANE, acute necrotizing encephalopathy.

For double immunofluorescence (IF), after antigen retrieval as described above, the sections were incubated in 0.1% Sudan black B/70% ethanol at 22–24 °C for 20 min to block autofluorescence. The sections were then incubated with polyclonal (for double IF with monoclonal anti-MAP2 or SMI31 antibody) or monoclonal (for double IF with polyclonal anti-SYP or AQP4 antibody) anti-GFAP antibody at 4°C overnight, followed by incubation with fluorescence-conjugated species-specific goat secondary antibodies (Alexa Fluor 488; Molecular Probes Inc., Eugene, OR, USA; 5 μg/mL) for 2 h at 22–24 °C. After several rinses in PBS, the sections were incubated with another primary antibody diluted in PBS containing 0.2% Triton-X 100 and 5% normal goat serum at 4 °C overnight, followed by incubation with the appropriate fluorescent-dye-conjugated secondary antibodies (Alexa Fluor 488, Alexa Fluor564; Molecular Probes; 5 μg/mL) for 2 h at 22–24 °C. After incubation with DAPI, the sections were mounted on slides and coverslipped with VECTASHIELD Mounting Medium (Vector Laboratories Inc.).

2.4. Confocal laser scanning microscopy

Confocal analysis was carried out using an LSM 510 META confocal laser scanning microscope (Carl Zeiss MicroImaging GmbH, Jena, Germany) and the LSM5 software. For the double staining of GFAP and autophagy markers, an LSM 710 and the ZEN software (Carl Zeiss) were used. Confocal images were acquired sequentially at 1 μm intervals through the z-axis of the mounted sections using the z-stack procedure and multitrack scanning function to avoid channel crosstalk. Individual optical planes and stacks of serial optical sections (projection images) were digitally recorded, and 3-dimensional (3D) images were reconstructed with the LSM or ZEN software.

2.5. Electron microscopy (EM)

Cerebellar sections from an IAE specimen (influenza #1) were used for EM studies. Unlabeled and GFAP-immunolabeled sections were processed to epon blocks. GFAP immunolabeling was performed using the ABC-DAB method described above. Afterward, the sections were fixed in 1% paraformaldehyde and 3% glutaraldehyde in 0.1 M phosphate buffer, postfixed in 1% osmium tetroxide, stained with 1% uranyl acetate, and embedded in Epon 812 (TAAB Laboratories Equipment Ltd., Berkshire, UK). After observation of semi-thin sections, ultra-thin sections were cut from them, stained with lead citrate, and observed under an H-7650 transmission electron microscope (Hitachi High-Technologies Co., Tokyo, Japan).

3. Results

3.1. Clasmatodendrosis was observed in multiple regions of all IAE brains

Immunostaining revealed that compared with the control (Fig. 1a, b), GFAP immunoreactivity in the IAE cerebrum and cerebellum (Fig. 1c–h) was markedly increased, especially in the cerebellar granular cell layer (GL; Fig. 1c), cerebellar WM, and cerebral WM (Fig. 1d). Furthermore, the astrocytic cytology in the IAE brains was highly unusual: the processes of GFAP-reactive astrocytes were highly fragmented, hav-

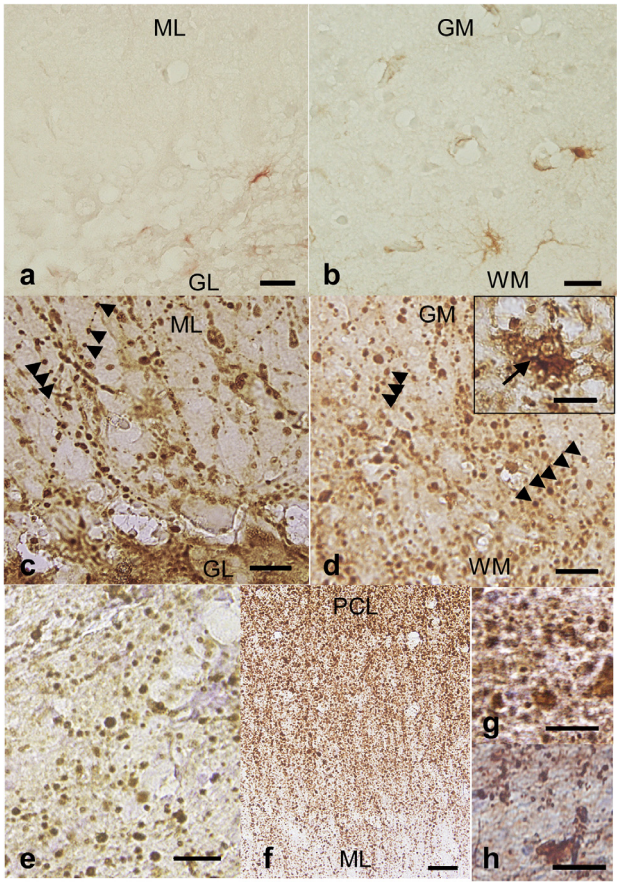

Fig. 1. Representative pictures of clasmatodendrosis in influenza-associated encephalopathy (IAE) brains. Glial fibrillary acidic protein (GFAP) immunostaining in the cerebellar cortex (a) and frontal cortex (b) of a non-IAE control brain and in the cerebellar cortex (c), frontal cortex (d), thalamus (e), hippocampus (f), splenium of the corpus callosum (g), and anterior commissure (h) of IAE brains. The swollen and vacuolated cell bodies of astrocytes (d, inset; the arrow indicates a vacuole, and arrowheads indicate the fragmented processes) in IAE brains were prominent in the white matter (WM) of the frontal lobe (d), corpus callosum (g), and anterior commissure (h); whereas the beading patterns were prominent in the cerebellar molecular layer (ML; b, arrowheads), cortico-medullary junction of the cerebrum (d, arrowheads), thalamus (e), and hippocampus (f). In e–h, nuclei were stained with Meyer's hematoxylin. ML, molecular layer; GL, granular layer; GM, gray matter; WM, white matter; PCL, pyramidal cell layer. Scale bars = 100 μm (a, b), 20 μm (c–f, h), 10 μm (inset in d), and 50 μm (g).

ing been transformed into strings of GFAP-positive granules ("strings of beads") in the cerebellar molecular layer (ML; arrowheads in Fig. 1c) and subcortical WM of the frontal lobe (arrowheads in Fig. 1d) in all 7 IAE brains. Most of these strings in the cerebellar ML were oriented radially, perpendicular to the Purkinje cell layer and cerebellar surface (arrowheads in Fig. 1c). The GFAP-positive astrocytes in the cerebral WM were swollen and vacuolated (arrow in the inset in Fig. 1d). Such swollen and vacuolated astrocytic cell bodies, together with their disintegrated processes, are the hallmark of clasmatodendrosis.

To investigate the distribution of clasmatodendrosis in IAE brains, we also performed GFAP immunostaining of other available brain regions, including the thalamus, hippocampus, and splenium of the corpus callosum – structures in which radiographic changes are frequently observed in IAE [1,3]. Variable degrees of clasmatodendrosis were detected in all examined regions (Fig. 1e–h); however, no signs of clasmatodendrosis could be detected in the corresponding regions of the available control brains (Table 2). The string-of-beads pattern of GFAP staining was especially prominent in the thalamus (Fig. 1e) and ML of the hippocampus (Fig. 1f).

3.2. Associations between GFAP-positive strings and other cellular structures in the cerebellar ML in IAE

To investigate the associations of degenerating astrocytic processes with specific brain structures, double immunohistochemistry staining of IAE brain sections was performed. Using SMI31 antibody, which recognizes phosphorylated neurofilaments as an axonal marker, we first examined the relationship between GFAP-positive bead strings and axons. In the cerebellum, SMI31 reactivity was observed in the deep ML running tangentially to the Purkinje cell layer and cerebellar surface, and perpendicular to the GFAP-positive strings (Fig. 2a–c). However, no obvious pattern between the SMI31- and GFAP-positive structures was detected (Fig. 2d–f).

Next, we examined the relationship between GFAP-positive bead strings and dendrites using MAP2 as a dendrite marker. GFAP-positive granules in the cerebellar ML of IAE brains appeared to co-localize with MAP2 (arrowheads in Fig. 2i). However, when the 3D images were rotated to demonstrate the fine positional relationship between the 2 sources of immunofluorescence, the MAP2 stained regions did not completely overlap with the GFAP stained regions (arrowheads in Fig. 2l), suggesting that the proteins were closely adjacent to each other but not co-localized. Because previous studies have revealed that MAP2 is localized in the dendritic spine as well as the dendritic shaft [22], the GFAP-positive beads may cap the MAP2-positive dendritic spines. In the cerebellar ML, the processes of Bergmann glia run in parallel with the MAP2-positive dendrites of Purkinje cells [22], ensheathing the dendritic spines [23]. In addition, the vertical growth of Purkinje cell dendrites occurs primarily in alignment with the processes of Bergmann glia [24], indicating that the GFAP-positive bead strings observed in IAE cerebella likely represent fragmented processes of Bergmann glia as opposed to the dendritic spines of Purkinje cells.

Similar to MAP2, immunochemical staining for SYP, a presynaptic marker, appeared to co-localize with GFAP-positive strings (arrowheads in Fig. 2o), but

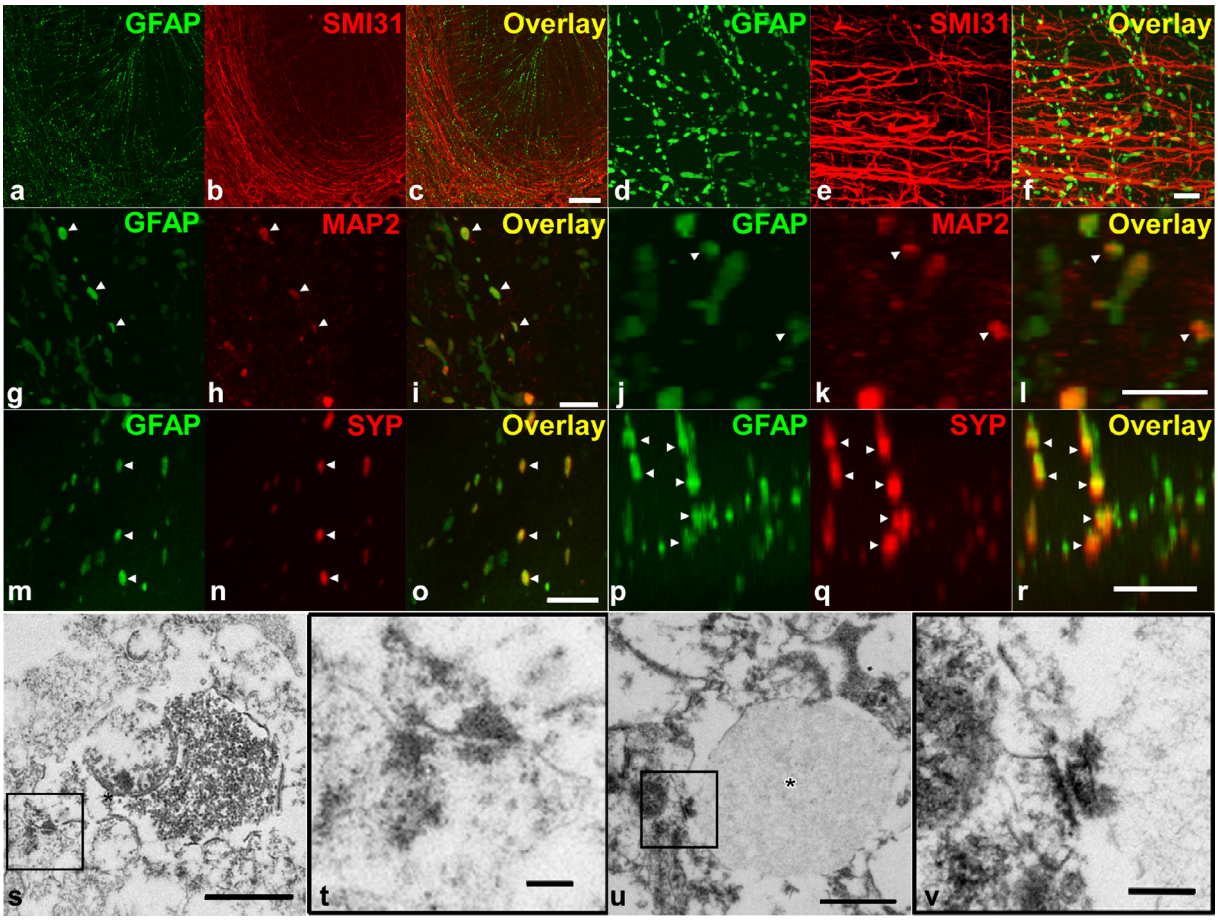

Fig. 2. Representative confocal images of double immunostaining for GFAP (green) and SMI31 (a–f), MAP2 (g–l), or SYP (m–r; all red) in the cerebellar cortices of IAE brains. GFAP-positive granules were not associated clearly with SMI31-antibody-reactive axons (c, f). MAP2 appeared to colocalize with GFAP-positive granules (arrowheads, i); however, when 3-dimensional reconstructed images were rotated and enhanced (j–l), the 2 signals did not overlap completely but, rather, were closely adjacent to each other (arrows, l). SYP-positive dots lay adjacent to GFAP-positive granules (o, arrowheads) and partially merged with them when 3-dimensional reconstructions were rotated (p–r, arrowheads in r). Electron micrographs (EM; s–v) of the cerebellar molecular layer in an IAE brain (influenza #1): s, GFAP-stained section; t, enlarged image of the boxed area in s; u, non-stained section; v, enlarged image of the boxed area in u. The astrocytic processes (indicated by asterisks), ascertained by GFAP immunolabeling, and the corresponding intermediate filaments were located adjacent to a synaptic structure (boxed in s,u and enlarged in t,v). GFAP, glial fibrillary acidic protein; GL, granular layer; IAE, influenza-associated encephalopathy; MAP2, microtubule-associated protein 2; ML, molecular layer; SYP, synaptophysin. Scale bars = 50 μm (a–c), 10 μm (d–r), 1 μm (s,u), and 0.2 μm (t,v).

was shown by rotation of 3D-reconstructed confocal images to be closely adjacent to, rather than completely overlapping, the GFAP-positive granules (arrowheads in Fig. 2r).

Next, we examined GFAP-positive astrocytic processes in IAE cerebella at the ultrastructural level (Fig. 2s–v). The cerebellum was chosen for further investigation because the string-of-beads pattern was most easily and clearly identified in the cerebellar ML. In GFAP-immunolabeled samples, the synapses (Fig. 2t, inset in Fig. 2s) and the immunoreactive processes of astrocytes (asterisk in Fig. 2s) were located adjacent to each other. Routine EM revealed the postsynaptic density (Fig. 2v, inset in Fig. 2u) adjacent to GFAP-positive astrocytic processes (asterisk in Fig. 2u), ruling out any artifactual dense staining of synaptic membranes. Although the EM samples were of poor quality, caused by long-term preservation of the autopsied brain in formalin, these findings support the association of fragmented astrocytic processes with synapses on the dendritic spines in the cerebellar ML of IAE brains. In GFAP-positive astrocytes, no isolation membranes or autophagosomes could be found, suggesting that autophagic processes were not involved in astrocyte clasmatodendrosis in IAE.

3.3. Clasmatodendrotic astrocytes in IAE did not colocalize with autophagy markers

Because previous reports have shown that clasmatodendrosis in rat models of status epilepticus represented astrocytic cell death by autophagy [16,17], we performed double IF staining with GFAP and autophagy markers (LC3 and p62) of IAE brains (Fig. 3). While some neu-

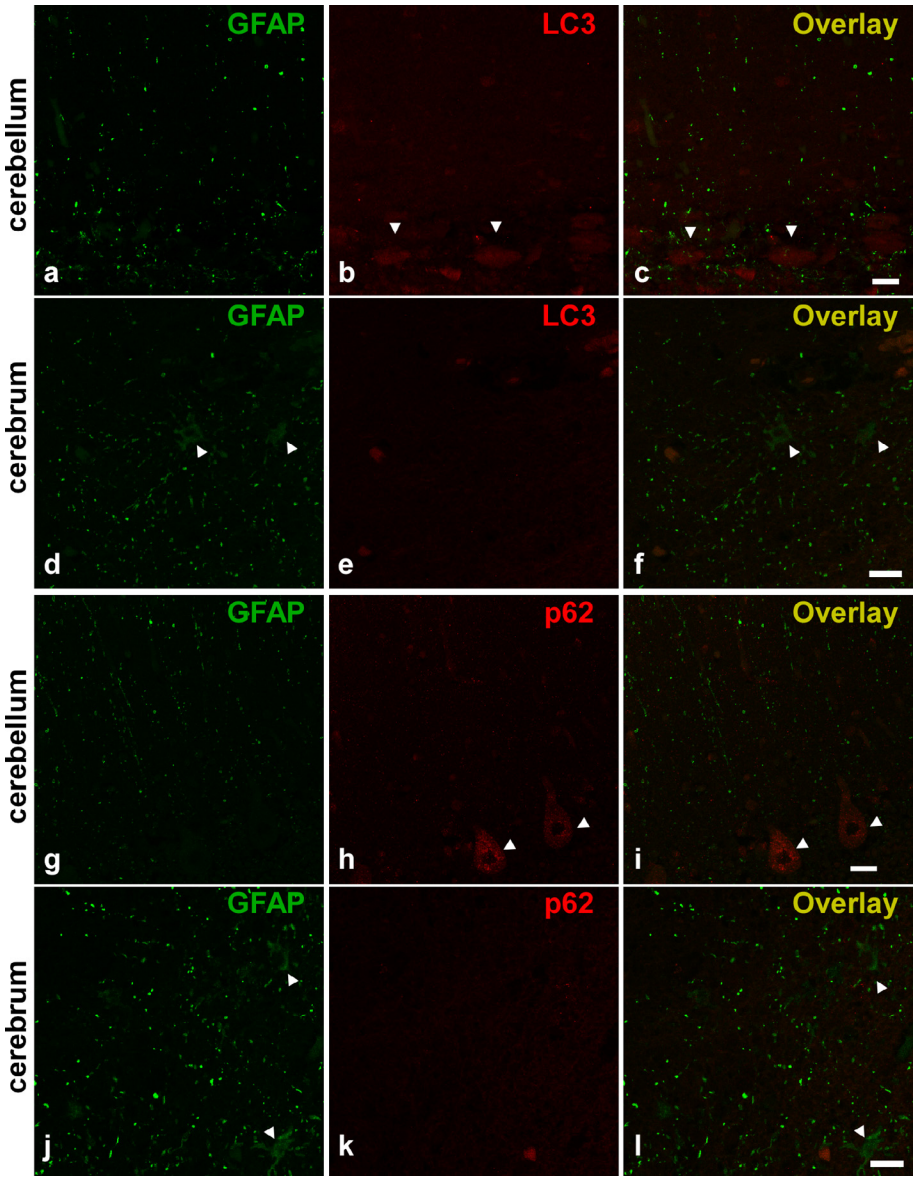

Fig. 3. Representative confocal images of double immunostaining for GFAP and autophagy markers in IAE brains. In the cerebellum, both the processes ("strings of beads") and cell bodies of clasmatodendrotic astrocytes were negative for LC3 (a–c) or p62 (g–i), while Purkinje cells (arrowheads in b,h) were positive for these autophagic markers. In the transitional zone between the GM and WM in the cerebrum (d–f, j–l), GFAP-positive astrocytes (arrowheads in d,j) were also negative for LC3 and p62 (arrowheads in f,l). GFAP, glial fibrillary acidic protein; GM, gray matter; IAE, influenza-associated encephalopathy; WM, white matter. Scale bars = 50 μm.

ronal somata, including those of Purkinje cells, in IAE cerebella showed LC3 (arrowheads in Fig. 3b) and p62 (arrowheads in Fig. 3h) signals, neither the cell bodies nor the beading processes of clasmatodendrotic astrocytes were positive for these markers (Fig. 3c,i). The GFAP-positive clasmatodendrotic astrocytes near the gray matter (GM)-WM border in the cerebrum (arrowheads in Fig. 3d,j) displayed no LC3 or p62 staining (arrowheads in Fig. 3f,l), while some neuronal somata in the GM were positive for these autophagic markers. Together with the absence of autophagic signs in astrocytes on EM examination, these results indicate that, unlike in status epilepticus, clasmatodendrosis in IAE is unlikely to be associated with autophagic astrocyte death.

3.4. Altered AQP4 distribution in IAE brains

The patterns of AQP4 immunoreactivity were different between control and IAE brains. In the control brains (Fig. 4a–c), intense AQP4 staining was present exclusively in the perivascular endfeet but not in the perisynaptic astrocytic processes. In contrast, in the IAE brains, AQP4 immunoreactivity was prominent in the clasmatodendrotic strings, but was decreased around the blood vessels (Fig. 4d–f). The GFAP-positive bead

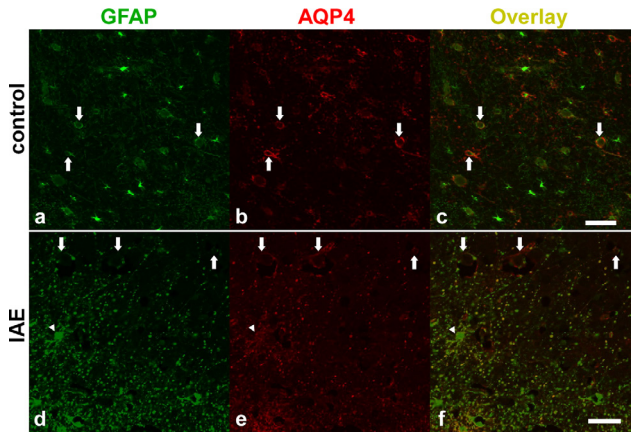

Fig. 4. Representative images of double immunostaining for GFAP (green) and AQP4 (red) in the cerebra of control (a–c) and IAE (d–f) brains. Blood vessels showed strong reactivity with antibody against AQP4 in the control brain (b, arrows), but only weak AQP4 reactivity in the IAE cerebrum (e, arrows). In addition, the beading processes of astrocytes in the IAE brain were positive for AQP4, as was the marginal areas of the astrocytic somata (e, arrowheads). AQP4, aquaporin 4; GFAP, glial fibrillary acidic protein; IAE, influenza-associated encephalopathy. Scale bars = 50 μm.

strings were also positive for AQP4 (Fig. 4f). Thus, the localization of AQP4 immunoreactivity appeared to change from perivascular astrocytic endfeet in the normal brains to fragmented perisynaptic astrocytic processes in the IAE brains.

3.5. Clasmatodendrosis in IAE brains was not associated with microglia activation

Since microglia play a major role in the inflammatory processes in the CNS, we performed immunostaining of microglia in IAE samples using anti-CD68 antibody. A wide variation in the degree of microglia activation and their number was observed among the IAE samples (data not shown), even though these samples showed equal extents of clasmatodendrosis. Although inflammatory cells had infiltrated into the meningeal regions in all of the IAE samples, the parenchyma of some IAE brains had few activated microglia, similar to the control brains. In contrast, clasmatodendrosis was detected in the parenchyma of all IAE brains, while being absent from the control brains (data not shown).

4. Discussion

In this study, we investigated the postmortem brains of 7 IAE patients and found clasmatodendrosis in all 7 brains. Clasmatodendrosis was present not only in the cerebral WM, the only site reported previously [10], but also in the cerebellum, thalamus, hippocampus, and splenium of the corpus callosum, where radiological changes are often found in different IAE subtypes [2,3]. The string-of-beads pattern of clasmatodendrosis was most prominent in the cerebellar ML, while also being present in other brain regions. This prominence was likely related to the structure of the cerebellar ML, where the astrocytes (i.e., Bergmann glia) cast long processes in 1 direction, perpendicular to the cerebellar surface, rather than reflecting selective involvement of the cerebellum.

Clasmatodendrosis has been described as an acute astrocytic reaction to energy failure and acidosis coupled with mitochondrial dysfunction [13,19]. Kim et al. showed that vacuolated astrocytes involved in clasmatodendrosis in the hippocampuses of epileptic rats were TdT-mediated dUTP Nick-End Labeling (TUNEL)-negative, whereas non-vacuolated astrocytes were TUNEL-positive [13,19]. Therefore, clasmatodendrosis has been considered to be an early stage of astrocyte necrosis [19]. However, recent studies in rat models of chronic status epilepticus have characterized clasmatodendrosis as resulting from autophagic astrocytic death [16,17]. In the present study, clasmatodendrotic astrocytes were not only negative for autophagic markers in immunofluorescence staining assays, but also lacking signs of autophagy on EM, suggesting that the mechanism of clasmatodendrosis in IAE is likely to be different from that in status epilepticus. We also performed a TUNEL assay on the IAE brains, and found that astrocytes undergoing clasmatodendrosis were TUNEL-negative (data not shown). Thus, clasmatodendrosis in IAE likely represents acute necrotic cell death of astrocytes. We could not detect necrosis in glial cells other than astrocytes, while only focal necrosis of neurons was observed. Further study is required to understand why diffuse necrotic changes in IAE are specific to astrocytes.

In our study, 2 of the 7 IAE cases (influenza #2 and 3) were diagnosed with Reye's syndrome without a history of aspirin administration. One case (influenza #5) showed obvious bilateral thalamic necrosis in both CT and pathological findings, which is characteristic of ANE. The other cases (influenza #1, 4, 6, and 7) were diagnosed as, or suspected to be, HSE based on the rapid clinical courses and laboratory data. It remains unclear whether clasmatodendrosis occurs in specific subtypes of IAE or is a feature of any rapidly progressive IAE, which is accompanied by severe acidosis. A case report recently described a case of rapidly progressing IAE without clasmatodendrosis or other histopathological findings usually detected in IAE [25], suggesting that the development of clasmatodendrosis does not immediately follow IAE onset.

To investigate factors associated with clasmatodendrosis further, we included brain tissues from patients who died of systemic inflammation diseases such as hemophagocytic syndrome and septic shock, which are

accompanied by hypercytokinemia and acidosis. These control brain samples had no signs of clasmatodendrosis in either the cerebrum or cerebellum. In addition, control patient #6, who died of suppurative encephalomyelitis with focal microscopic abscesses, also showed no clasmatodendrosis, whereas activated astrocytes were present. These results suggest that local brain infection, systemic inflammation, and hypercytokinemia are not sufficient to induce clasmatodendrosis. It is likely that genetic vulnerability or other additional factors are needed to develop IAE [26]. However, the exact mechanism of IAE pathogenesis remains to be established.

Do astrocytic processes become fragmented randomly or in response to extra- or intracellular cues? Using single-cell cultures of hippocampal astrocytes maintained under hyperglycemic and acidic conditions, Hulse et al. [27] demonstrated that clasmatodendrosis could occur without neuronal interaction. However, we found that fragmented astrocytic processes corresponded to synaptic complexes *in vivo*. It is possible that, in the IAE brain, excess water and electrolytes tend to accumulate at astrocytic processes near synapses, where the neuron-astrocyte interaction is intensive, to maintain normal transmission, which may induce selective fragmentation in the perisynaptic area.

AQP4, a key molecule for maintaining the water balance in the brain, is mainly expressed in the endfeet of astrocytes around blood vessels (perivascularly) and is thought to be a component of the BBB [28]. AQP4 is expressed in astrocytic processes around synapses as well [28]. Multiple studies have shown that AQP4 dysfunction or structural damage causes cytotoxic edema [21,28]. Recent studies have also demonstrated that AQP4 expression is downregulated in anoxia and chronic epilepsy in rats, suggesting that decreased AQP4 levels may play a protective role in brain edema [13,19]. In addition, our study revealed that, while perisynaptic astrocytic processes and somata showed increased AQP4 expression, perivascular processes displayed decreased AQP4 levels in IAE-associated clasmatodendrosis. Such displacement of AQP4 was also reported in clasmatodendrosis in post-stroke dementia [20] and an animal model of hypoperfusion [12]. The breakdown of the astrocytic processes in IAE brains may interrupt the siphoning of water taken up by AQP4 at the synapse into the blood. One possible explanation for the altered AQP4 distribution is that the mechanisms keeping AQP4 concentrated and anchored to the perivascular domains of astrocytes, such as the one involving α-syntrophin [21,28], may become dysfunctional. Such dysfunction may impair the normal synaptic transmission and trigger the development of IAE. Alternatively, at an early phase, the increased perisynaptic AQP4 levels may function to maintain homeostasis in the synaptic complex while AQP4 scarcity in the perivascular astrocytes alleviates brain edema. This compensatory mechanism would break down at the commencement of the fragmentation of astrocytic processes.

The major limitation of our study is that the diagnosis of IAE was confirmed by direct detection of viral antigen in only 3 of the 7 cases. Before the development and spread of rapid testing methods to detect influenza virus antigen around the year 2000, influenza infection was mostly diagnosed by the presence of clinical symptoms and concurrence with an epidemic. The most reliable method to confirm the diagnosis of influenza infection is to detect viral antigen by PCR; however, it has not been applied to all suspected IAE cases, particularly in the early days. Our sample included patients who died before the development of rapid testing methods, when viral detection was not routinely performed. Another limitation of IAE studies, including ours, is the small number of available samples. After the development of anti-viral agents for influenza, the progress in supportive care for IAE and the formulation of the Guidelines for IAE by the Japanese Ministry of Health, Labor, and Welfare in 2005 [29] have led to the drastic decrease in the IAE mortality rate from approximately 30% to 7% [7]. The number of autopsied patients with IAE has declined accordingly. Although this decrement is a welcome development, it makes it more difficult to investigate the neuropathology of new IAE cases. Therefore, the results of the present study are all the more valuable. However, the incidence of IAE has not decreased, and even now, more than 10% of the affected patients in Japan suffer sequelae such as quadriplegia and psychoneurotic dysfunction [8], making detailed investigations of the IAE pathology necessary for the prevention and alleviation of IAE.

Another limitation of this study is that our control group did not include cases of non-influenza acute encephalopathy or influenza infection without acute encephalopathy. Therefore, it remains unclear whether influenza or acute encephalopathy causes the clasmatodendrotic changes in astrocytes in IAE brains. Our preliminary search of the autopsy records at 2 institutes revealed that clasmatodendrosis was present in18 autopsied brains, 17 of which were from patients with acute encephalopathies, including 12 patients with IAE. Thus, while clasmatodendrosis may occur in acute encephalopathies caused by pathogens other than influenza, it is detected most frequently in IAE brains, suggesting that diffuse clasmatodendrosis may be a suggestive pathological feature of IAE.

In conclusion, this study demonstrated the presence of clasmatodendrosis in most regions of IAE brains. Clasmatodendrotic astrocyte processes appeared prominently as GFAP-positive bead strings closely associated with synapses. Furthermore, clasmatodendrosis in astrocytes in IAE was not associated with autophagy. We also demonstrated an altered AQP4 distribution in

IAE brains and showed its relationship to clasmatodendrosis. Based on our results, we speculate that synaptic dysfunction in IAE may result from the perturbation of perisynaptic astrocytes. Further evidence on the molecular mechanisms of clasmatodendrosis in IAE is required to clarify the pathophysiology of IAE and develop approaches to prevent the irreversible astrocytic degeneration, thus improving patient outcomes.

Acknowledgements

The authors thank Drs. Toshiyuki Mano, Yuri Etani, and Hitoshi Tajiri at Osaka General Medical Center for providing the IAE samples. We also thank Dr. Kinuko Suzuki at Tokyo Metropolitan Geriatric Hospital & Institute of Gerontology and Dr. Keiko Taya at the National Institute of Infectious Diseases for their helpful comments on this manuscript, Dr. Hiroyuki Hatsuda at Tokyo Metropolitan Institute of Gerontology and Dr. Masako Ikemura at the University of Tokyo Hospital for their cooperation in collecting clasmatodendrotic brain samples. We also appreciate Ms. Masami Nakamura's excellent technical support. This study was supported in part by research grants from the Ministry of Education, Culture, Sports, Science, and Technology of Japan (grant no. 22591126 to I.M.).

References

[1] Sugaya N. Influenza-associated encephalopathy in Japan: pathogenesis and treatment. Pediatr Int 2000;42:215–8.
[2] Togashi T, Matsuzono Y, Narita M, Morishima T. Influenza-associated acute encephalopathy in Japanese children in 1994–2002. Virus Res 2004;103:75–8.
[3] Mizuguchi M, Yamanouchi H, Ichiyama T, Shiomi M. Acute encephalopathy associated with influenza and other viral infections. Acta Neurol Scand 2007;115:45–56.
[4] Morishima T, Togashi T, Yokota S, Okuno Y, Miyazaki C, Tashiro M, et al. Encephalitis and encephalopathy associated with an influenza epidemic in Japan. Clin Infect Dis 2002;35:512–7.
[5] Lyon JB, Remigio C, Milligan T, Deline C. Acute necrotizing encephalopathy in a child with H1N1 influenza infection. Pediatr Radiol 2010;40:200–5.
[6] Ormitti F, Ventura E, Summa A, Picetti E, Crisi G. Acute necrotizing encephalopathy in a child during the 2009 influenza A (H1N1) pandemia: MR imaging in diagnosis and follow-up. AJNR Am J Neuroradiol 2010;31:396–400.
[7] Hoshino A, Saitoh M, Oka A, Okumura A, Kubota M, Saito Y, et al. Epidemiology of acute encephalopathy in Japan, with emphasis on the association of viruses and syndromes. Brain Dev 2012;34:337–43.
[8] Kawashima H, Morichi S, Okumara A, Nakagawa S, Morishima T. National survey of pandemic influenza A (H1N1) 2009-associated encephalopathy in Japanese children. J Med Virol 2012;84:1151–6.
[9] Wang GF, Li W, Li K. Acute encephalopathy and encephalitis caused by influenza virus infection. Curr Opin Neurol 2010;23:305–11.
[10] Tomimoto H, Akiguchi I, Wakita H, Suenaga T, Nakamura S, Kimura J. Regressive changes of astroglia in white matter lesions in cerebrovascular disease and Alzheimer's disease patients. Acta Neuropathol 1997;94:146–52.
[11] Sahlas DJ, Bilbao JM, Swartz RH, Black SE. Clasmatodendrosis correlating with periventricular hyperintensity in mixed dementia. Ann Neurol 2002;52:378–81.
[12] Hase Y, Craggs L, Hase M, Stevenson W, Slade J, Lopez D, et al. Effects of environmental enrichment on white matter glial responses in a mouse model of chronic cerebral hypoperfusion. J Neuroinflammation 2017;14:81.
[13] Kim JE, Ryu HJ, Yeo SI, Kang TC. P2X7 receptor differentially modulates astroglial apoptosis and clasmatodendrosis in the rat brain following status epilepticus. Hippocampus 2011;21:1318–33.
[14] Ohama E, Miyata H, Otsuka M, Kimura N, Tanaka Y, Yamashita S, et al. Clasmatodendrosis in acute encephalopathies: an immunohistochemical study (in Japanese). Neuropathology 2004;24:A42.
[15] Yoshimura H, Imai Y, Beppu M, Ohara N, Kobayashi J, Kuzuya A, et al. Elderly autopsy case of influenza-associated encephalopathy (in Japanese). Rinsho Shinkeigaku 2008;48:713–20.
[16] Ryu HJ, Kim JE, Yeo SI, Kang TC. p65/RelA-Ser529 NF-kappaB subunit phosphorylation induces autophagic astroglial death (Clasmatodendrosis) following status epilepticus. Cell Mol Neurobiol 2011;31:1071–8.
[17] Kim JE, Hyun HW, Min SJ, Kang TC. Sustained HSP25 Expression Induces Clasmatodendrosis via ER Stress in the Rat Hippocampus. Front Cell Neurosci 2017;11:47.
[18] Sugawara T, Lewen A, Noshita N, Gasche Y, Chan PH. Effects of global ischemia duration on neuronal, astroglial, oligodendroglial, and microglial reactions in the vulnerable hippocampal CA1 subregion in rats. J Neurotrauma 2002;19:85–98.
[19] Kim JE, Ryu HJ, Yeo SI, Seo CH, Lee BC, Choi IG, et al. Differential expressions of aquaporin subtypes in astroglia in the hippocampus of chronic epileptic rats. Neuroscience 2009;163:781–9.
[20] Chen A, Akinyemi RO, Hase Y, Firbank MJ, Ndung'u MN, Foster V, et al. Frontal white matter hyperintensities, clasmatodendrosis and gliovascular abnormalities in ageing and post-stroke dementia. Brain 2016;139:242–58.
[21] Amiry-Moghaddam M, Otsuka T, Hurn PD, Traystman RJ, Haug FM, Froehner SC, et al. An alpha-syntrophin-dependent pool of AQP4 in astroglial end-feet confers bidirectional water flow between blood and brain. Proc Natl Acad Sci U S A 2003;100:2106–11.
[22] Matus A, Delhaye-Bouchaud N, Mariani J. Microtubule-associated protein 2 (MAP2) in Purkinje cell dendrites: evidence that factors other than binding to microtubules are involved in determining its cytoplasmic distribution. J Comp Neurol 1990;297:435–40.
[23] Lippman JJ, Lordkipanidze T, Buell ME, Yoon SO, Dunaevsky A. Morphogenesis and regulation of Bergmann glial processes during Purkinje cell dendritic spine ensheathment and synaptogenesis. Glia 2008;56:1463–77.
[24] Lordkipanidze T, Dunaevsky A. Purkinje cell dendrites grow in alignment with Bergmann glia. Glia 2005;51:229–34.
[25] Nara A, Nagai H, Yamaguchi R, Yoshida K, Iwase H, Mizuguchi M. An unusual autopsy case of cytokine storm-derived influenza-associated encephalopathy without typical histopathological findings: autopsy case report. Am J Forensic Med Pathol 2015;36:3–5.
[26] Yao M, Yao D, Yamaguchi M, Chida J, Kido H. Bezafibrate upregulates carnitine palmitoyltransferase II expression and promotes mitochondrial energy crisis dissipation in fibroblasts of patients with influenza-associated encephalopathy. Mol Genet Metab 2011;104:265–72.

[27] Hulse RE, Winterfield J, Kunkler PE, Kraig RP. Astrocytic clasmatodendrosis in hippocampal organ culture. Glia 2001;33:169–79.
[28] Amiry-Moghaddam M, Ottersen OP. The molecular basis of water transport in the brain. Nat Rev Neurosci 2003;4:991–1001.
[29] The Research Committee on the Clarification of Etiology and on the Establishment of Therapeutic and Preventive Measures of Influenza Encephalopathy. Guideline for influenza encephalopathy [in Japanese]. Japanese Ministry of Health, Labor and Welfare; 2005:1–21.